



ELSEVIER

15 July 2001

Optics Communications 194 (2001) 289–297

---

---

OPTICS  
COMMUNICATIONS

---

---

www.elsevier.com/locate/optcom

# Fast Fourier factorization method applied to modal analysis of slanted lamellar diffraction gratings in conical mountings

B. Chernov<sup>a</sup>, M. Nevière<sup>b</sup>, E. Popov<sup>b,\*</sup>

<sup>a</sup> Department of Optical and Quantum Radiophysics, State University of Telecommunications, St. Petersburg 191186, Russia

<sup>b</sup> Institut Fresnel, Unité Mixte de Recherche du Centre National de la Recherche Scientifique N° 6133, Faculté des Sciences et Techniques de St-Jérôme, 13397 Marseille Cedex 20, France

Received 14 February 2001; accepted 16 May 2001

---

## Abstract

A new formulation of the Fourier modal method that applies fast Fourier factorization [J. Opt. Soc. Am. A 17 (2000) 1773] is presented for slanted lamellar gratings in conical mountings. A new eigenvalue problem in the grating region is derived, and used to study metallic gratings. Comparison of the convergence speed of the numerical results given by the conventional methods and the new one shows a spectacular improvement. The fast Fourier factorization method can be also applied to various volume slanted-fringe gratings with discontinuous permittivity variations. © 2001 Elsevier Science B.V. All rights reserved.

*Keywords:* Diffraction; Diffraction gratings; Fourier factorization

---

## 1. Introduction

Recently, the differential theory of gratings was revised with fast Fourier factorization method (FFFM) [1]. A strong improvement of the convergence was obtained for TM polarization. Developed in paper [1] FFFM is applicable to any theory that requires the Fourier analysis of continuous products of discontinuous periodic functions. This paper is aimed at improving the convergence of the Fourier modal method (FMM) [2] for slanted lamellar gratings in conical mountings. In the FMM (also known as the modal method by Fourier expansion [3–6], the rigorous coupled-wave method [7–13], and the rigorous characteristic wave method [14,15]), both the electromagnetic fields and the permittivity function are expanded into Fourier series. However in conventional formulation FMM slowly converges for metallic gratings in TM polarization [9]. Recent papers [11,12] proposed a reformulation of the propagation equations and the eigenvalue problem in the grating region, which constituted great progress for unslanted lamellar gratings. The remarkable work of Li [16] provided mathematical foundation for a new formulation of the FMM. Using three theorems of Fourier factorization, Li established the following extremely important conclusion:

---

\* Corresponding author. Fax: +33-4-9167-4428.

E-mail address: evgueni.popov@fresnel.fr (E. Popov).

Although the equations of the original modal theory were exact – both those written in spatial variables and those in discrete Fourier space – the latter ones become ill-suited when truncated by any numerical treatment. Li proposed appropriate factorization rules to avoid this problem. In paper [1] these rules were used to establish new propagation equations for the differential method that can be truncated without any numerical problems. These equations were established for arbitrary profiles for TM polarization in planar (nonconical) mountings.

In this paper for the general case of conical mountings, the FFFM is used for modal analysis of volume and/or surface-relief slanted-fringe gratings with discontinuous permittivity variations. Numerical results are given for most interesting particular case of metallic slanted lamellar diffraction gratings. A comparison of the convergence speed of the numerical results given by the conventional methods and the FFFM based method is made.

## 2. Modal solution in the grating region

The geometry of grating diffraction problem in conical mountings is depicted in Fig. 1 for the particular case of surface-relief slanted lamellar diffraction grating.

In the present analysis, without any loss of generality, the following geometry is used: (1) grating vector  $\mathbf{K}$  is in the  $xz$  plane, (2) the boundary normal is in the  $z$  direction, (3) the plane of incidence, that is formed by incident wave vector  $\mathbf{k}_1$  and the  $z$ -axis, makes an angle  $\delta$  with respect to the  $x$ -axis as shown in Fig. 1. A linearly polarized electromagnetic wave is obliquely incident at an arbitrary angle  $\theta$  on a slanted-fringe mixed amplitude and phase planar grating of slant angle  $\alpha$  bounded by two different media. The superstratum and the substrate (regions 1 and 3) are homogeneous with relative permittivities  $\epsilon_1$  and  $\epsilon_2$ , respectively. In the grating region (region 2,  $0 < z < b$ ) permittivity  $\epsilon$  is modulated periodically along grating vector  $\mathbf{K}$ ,

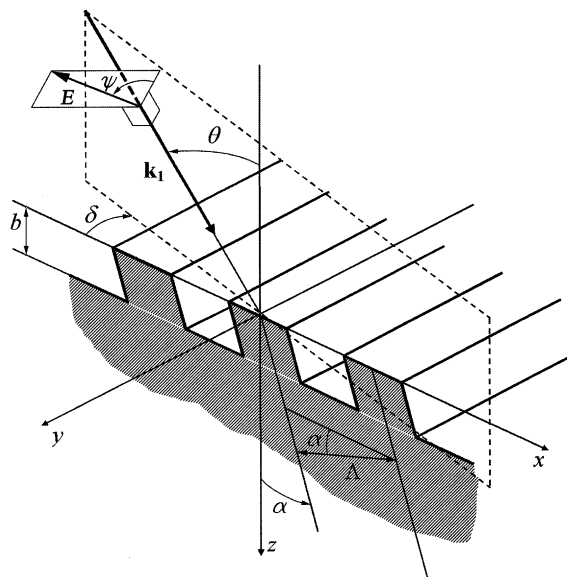


Fig. 1. Geometry of a grating diffraction problem in conical mountings for the particular case of surface-relief slanted lamellar diffraction grating.

$$\varepsilon(x, z) = \sum_m \varepsilon_m \exp(im\mathbf{K} \cdot \mathbf{r}), \tag{1}$$

where  $\varepsilon_m$  is the  $m$ th Fourier component of the complex relative permittivity  $\varepsilon$ ,

$$\mathbf{K} = K_x \hat{\mathbf{x}} + K_z \hat{\mathbf{z}}, \quad K_x = K \cos \alpha, \quad K_z = -K \sin \alpha, \quad K = 2\pi/\Lambda,$$

$\hat{\mathbf{x}}, \hat{\mathbf{y}}, \hat{\mathbf{z}}$  are unit vectors, and  $\Lambda$  is the grating period.

In region 1, the incident normalized electric-field vector is

$$\mathbf{E}_0 = \hat{\mathbf{u}} \exp(-i\mathbf{k}_1 \cdot \mathbf{r}), \tag{2}$$

with

$$\begin{aligned} \mathbf{k}_1 &= k_x \hat{\mathbf{x}} + k_y \hat{\mathbf{y}} + k_{1z} \hat{\mathbf{z}}, \quad k_x = k_1 \sin \theta \cos \delta, \quad k_y = k_1 \sin \theta \sin \delta, \\ k_{1z} &= k_1 \cos \theta, \quad k_1^2 = k_0^2 \varepsilon_1, \quad k_0 = 2\pi/\lambda, \end{aligned} \tag{3}$$

$\lambda$  is the free-space wavelength, and  $\hat{\mathbf{u}}$  is the polarization unit vector given by

$$\begin{aligned} \hat{\mathbf{u}} &= u_x \hat{\mathbf{x}} + u_y \hat{\mathbf{y}} + u_z \hat{\mathbf{z}}, \quad u_x = \cos \psi \cos \theta \cos \delta - \sin \psi \sin \delta, \quad u_y = \cos \psi \cos \theta \sin \delta + \sin \psi \cos \delta, \\ u_z &= -\cos \psi \sin \theta, \end{aligned} \tag{4}$$

where  $\psi$  is the angle between the polarization vector and the plane of incidence.

For  $\psi = 0^\circ$  and  $\psi = 90^\circ$ , the magnetic field vector and the electric field vector, respectively, are perpendicular to the plane of incidence.

In the grating region 2 ( $0 < z < b$ ), Maxwell's equations are expressed as

$$\nabla \times \mathbf{E} = -i\omega\mu_0 \mathbf{H}, \quad \nabla \times \mathbf{H} = i\omega\varepsilon_0 \varepsilon(\mathbf{r}) \mathbf{E}. \tag{5}$$

The time dependence of all field quantities is assumed to be of the form  $\exp(i\omega t)$ ,  $\omega$  is the angular frequency of the incident electromagnetic plane wave;  $\mu_0$  is the permeability of free space, which is assumed to be the same in all regions.

From the phase matching conditions and the theory of sets of differential equations with periodic coefficients it follows that in the modulated region (region 2) the electric and magnetic fields may be expressed as expansions in the terms of modes as

$$\mathbf{E}_2 = \sum_q A_q \mathbf{E}_q, \quad \mathbf{H}_2 = \sum_q A_q \mathbf{H}_q, \tag{6}$$

$$\begin{aligned} \mathbf{E}_q &= \sum_j E_{jq} \hat{\mathbf{j}}, \quad \mathbf{H}_q = \sum_j H_{jq} \hat{\mathbf{j}}, \quad E_{jq} = \sum_n e_{njq} \exp[-i(k_{nx}x + k_y y - \mathcal{K}_{nq}z)], \\ H_{jq} &= (\varepsilon_0/\mu_0)^{1/2} \sum_n h_{njq} \exp[-i(k_{nx}x + k_y y - \mathcal{K}_{nq}z)], \end{aligned} \tag{7}$$

where mode numbers are  $q = 1, 2, 3, \dots$ , mode amplitudes  $A_q$  are unknown constants to be determined from boundary conditions,  $\hat{\mathbf{j}}$  ( $\hat{\mathbf{j}} = \hat{\mathbf{x}}, \hat{\mathbf{y}}, \hat{\mathbf{z}}$ ) is the unit vector along the  $\mathbf{j}$ -axis,  $n = 0, \pm 1, \pm 2, \pm 3, \dots$ ,

$$k_{nx} = k_x - nK_x, \quad \mathcal{K}_{nq} = P_q K + nK_z, \tag{8}$$

and  $P_q$  are unknown parameters corresponding to the  $q$  particular solution of the Eq. (5). Note that, if the total number of space harmonics retained in Rayleigh expansion in the superstratum region is  $(2N + 1)$  and the same number is in the substrate region also, then  $(2N + 1)$  pseudo-Fourier harmonics have to be retained in the field expansion (7) and  $n = 0, \pm 1, \pm 2, \pm 3, \dots, \pm N$ ,  $q = 1, 2, 3, \dots, 4(2N + 1)$ .

Throughout the paper, we use the subscripts  $i, j$  as coordinate indices, and the subscripts  $q$  as the particular solution of Eq. (5) indices. For convenience,  $q$  subscripts will be henceforth suppressed unless otherwise stated.

### 3. Reformulation of the eigenproblem with fast Fourier factorization method

In accordance with FFFM we consider the  $E_x$  and  $E_z$  components of the field in the grating region in terms of tangential  $E_T$  and the normal  $E_N$  components

$$\begin{aligned} E_T &= E_x \sin \alpha + E_z \cos \alpha, \\ E_N &= E_x \cos \alpha - E_z \sin \alpha, \end{aligned} \quad (9)$$

Inverting Eq. (9) leads to

$$\begin{aligned} E_x &= sE_T + cE_N, \\ E_z &= cE_T - sE_N, \end{aligned} \quad (10)$$

where following abbreviations are used:

$$s = \sin \alpha, \quad c = \cos \alpha.$$

The right-hand side of the second equation of Eq. (5) contains product  $\varepsilon \mathbf{E}$  with components

$$\varepsilon E_x = s\varepsilon E_T + c\varepsilon E_N, \quad (11)$$

$$\varepsilon E_z = c\varepsilon E_T - s\varepsilon E_N. \quad (12)$$

The  $E_y$  and  $E_T$  components are tangential to the surface of permittivity discontinuities in grating region and, thus they are continuous functions. The product  $\varepsilon E_y$  and the first term on the right-hand side in Eqs. (11) and (12),  $\varepsilon E_T$ , include the product of the discontinuous function  $\varepsilon$  by continuous functions  $E_y$  and  $E_T$ , respectively. Following conclusion 1 of Li [16], the Fourier components of the products  $\varepsilon E_y$  and  $\varepsilon E_T$  can be found through the Laurent's rule. Although  $\varepsilon$  and  $E_N$  are discontinuous, the product  $\varepsilon E_N$  in Eqs. (11) and (12) is continuous (since it is proportional to the component of  $\mathbf{D}$  normal to the surface of permittivity discontinuities in grating region). Thus the calculation of the Fourier components of the product  $\varepsilon E_N$  requires the use of conclusion 2 of Li [16], i.e. the use of the inverse rule.

We then get

$$[\varepsilon e_x] = s \|\varepsilon\| [e_T] + c \left\| \frac{1}{\varepsilon} \right\|^{-1} [e_N], \quad (13)$$

$$[\varepsilon e_y] = \|\varepsilon\| [e_y], \quad (14)$$

$$[\varepsilon e_z] = c \|\varepsilon\| [e_T] - s \left\| \frac{1}{\varepsilon} \right\|^{-1} [e_N], \quad (15)$$

where  $[e_i]$  denotes the vector constructed with the pseudo-Fourier coefficients of  $E_i$  such that its  $m$  entry is  $e_{mi}$ ,  $\|\varepsilon\|$  denotes the Toeplitz matrix generated by the Fourier coefficients of  $\varepsilon$  such that its  $(n, m)$  entry is  $\varepsilon_{n-m}$ , superscript  $-1$  denotes the matrix inverse, and

$$\frac{1}{\varepsilon(x, z)} = \sum_m \left( \frac{1}{\varepsilon} \right)_m \exp(im\mathbf{K} \cdot \mathbf{r}). \quad (16)$$

Substituting Eq. (9) into Eqs. (13) and (15), we find

$$[\varepsilon e_x] = \mathbf{A}[e_x] + \mathbf{B}[e_z], \tag{17}$$

$$[\varepsilon e_z] = \mathbf{B}[e_x] + \left( c^2 \|\varepsilon\| + s^2 \left\| \frac{1}{\varepsilon} \right\|^{-1} \right) [e_z], \tag{18}$$

where

$$\mathbf{A} = s^2 \|\varepsilon\| + c^2 \left\| \frac{1}{\varepsilon} \right\|^{-1}, \quad \mathbf{B} = sc \left( \|\varepsilon\| - \left\| \frac{1}{\varepsilon} \right\|^{-1} \right), \tag{19}$$

From Eq. (18), it follows that

$$[e_z] = \mathbf{G}([\varepsilon e_z] - \mathbf{B}[e_x]), \tag{20}$$

where

$$\mathbf{G} = \left( c^2 \|\varepsilon\| + s^2 \left\| \frac{1}{\varepsilon} \right\|^{-1} \right)^{-1}, \tag{21}$$

The product  $\varepsilon E_z$  can be obtained from Maxwell's equations (5)

$$\varepsilon E_z = -\frac{i}{\omega \varepsilon_0} \left( \frac{\partial H_y}{\partial x} - \frac{\partial H_x}{\partial y} \right), \tag{22}$$

Substituting expansions for  $E_j$  and  $H_j$  from Eq. (7) into Eq. (22), we find in the Fourier space

$$[\varepsilon e_z] = -\mathbf{k}[h_y] + \mathbf{k}_{y0}[h_x], \tag{23}$$

where  $\mathbf{k}$  is a diagonal matrix, with diagonal elements  $k_{nx}/k_0$ ,  $\mathbf{k}_{y0} = \left( \frac{k_y}{k_0} \right) \mathbf{I}$ , and  $\mathbf{I}$  is the identity matrix.

Substituting Eq. (23) into Eq. (20), we find

$$[e_z] = \mathbf{G}(\mathbf{k}_{y0}[h_x] - \mathbf{k}[h_y] - \mathbf{B}[e_x]). \tag{24}$$

From Eqs. (17) and (24), it follows that

$$[e_x] = (\mathbf{A} - \mathbf{BGB})[e_x] + \mathbf{BGk}_{y0}[h_x] - \mathbf{BGk}[h_y]. \tag{25}$$

Substituting Eqs. (7), (14), (24) and (25) into Maxwell's equations (5) and eliminating  $e_{nz}$  and  $h_{nz}$  components of the field, we obtain the set of algebraic equations in a matrix form:

$$(\mathbf{W} - P\mathbf{I})[g] = 0, \tag{26}$$

where

$$\mathbf{W} = -\frac{k_0}{K} \begin{pmatrix} \mathbf{S} & -\mathbf{k}_{y0}\mathbf{GB} & -\mathbf{k}_{y0}\mathbf{Gk} & (\mathbf{k}_{y0}^2\mathbf{G} - \mathbf{I}) \\ 0 & (\mathbf{S} - \mathbf{kGB}) & (\mathbf{I} - \mathbf{kGk}) & \mathbf{kGk}_{y0} \\ \mathbf{k}_{y0}\mathbf{k} & (\mathbf{A} - \mathbf{BGB} - \mathbf{k}_{y0}^2) & (\mathbf{S} - \mathbf{BGk}) & 0 \\ (\mathbf{k}^2 - \|\varepsilon\|) & \mathbf{k}\mathbf{k}_{y0} & 0 & \mathbf{S} \end{pmatrix}, \quad [g] = \begin{bmatrix} e_y \\ e_x \\ h_y \\ h_x \end{bmatrix}. \tag{27}$$

In Eq. (27), each element of the column vector  $[g]$  is itself a column vector  $[e_j]$  or  $[h_j]$ , and  $\mathbf{S}$  is a diagonal matrix, with the  $(n, n)$  element being equal to  $nK_z/k_0$ .

In order to solve the linear system equation (26) on a computer, we have to truncate the matrices. Submatrices in the matrix  $\mathbf{W}$  are  $(2N + 1) \times (2N + 1)$  matrices, where  $(2N + 1)$  is the number of pseudo-Fourier harmonics retained in the field expansion (7), with the  $n$ th row of the submatrix corresponding to

the  $n$ th harmonic. Thus, the matrix  $\mathbf{W}$  is  $4 \times (2N + 1)$  by  $4 \times (2N + 1)$  square matrix, and Eq. (26) has the form of eigenvalue equation. A numerical solution of the eigenvalue problem, Eq. (26), gives  $4 \times (2N + 1)$  eigenvalues  $P_q$  and eigenvectors  $[g_q]$ . According to Eq. (6) the fields in the grating region may be written as a superposition of eigenmodes with unknown coefficients  $A_q$ , where  $q = 1, 2, 3, \dots, 4 \times (2N + 1)$ .

The diffracted fields outside the grating region may be expressed in the form of Rayleigh expansions. The amplitudes of the diffracted fields together with  $A_q$  are calculated by matching the tangential electric and magnetic fields at the two boundaries of the modulated region ( $z = 0$  and  $z = b$ ).

#### 4. Comparison with the previous formulations

In the conventional formulation [3–9] the Laurent's rule is used

$$\begin{aligned} [\varepsilon e_x] &= \|\varepsilon\| [e_x], \\ [e_z] &= \left\| \frac{1}{\varepsilon} \right\| (\mathbf{k}_{y0} [h_x] - \mathbf{k} [h_y]), \end{aligned} \quad (28)$$

and

$$\mathbf{W} = -\frac{k_0}{K} \begin{pmatrix} \mathbf{S} & 0 & -\mathbf{k}_{y0} \|\frac{1}{\varepsilon}\| \mathbf{k} & (\mathbf{k}_{y0}^2 \|\frac{1}{\varepsilon}\| - \mathbf{I}) \\ 0 & \mathbf{S} & (\mathbf{I} - \mathbf{k} \|\frac{1}{\varepsilon}\| \mathbf{k}) & \mathbf{k} \|\frac{1}{\varepsilon}\| \mathbf{k}_{y0} \\ \mathbf{k}_{y0} \mathbf{k} & (\|\varepsilon\| - \mathbf{k}_{y0}^2) & \mathbf{S} & 0 \\ (\mathbf{k}^2 - \|\varepsilon\|) & \mathbf{k} \mathbf{k}_{y0} & 0 & \mathbf{S} \end{pmatrix}. \quad (29)$$

A comparison of Eq. (28) with Eqs. (17) and (24) shows that matrix  $\mathbf{W}$  in conventional formulation (Eq. (29)) may be obtained from Eq. (27), if

$$\mathbf{A} = \|\varepsilon\|, \quad \mathbf{B} = 0, \quad \mathbf{G} = \left\| \frac{1}{\varepsilon} \right\|. \quad (30)$$

In paper [10] the conventional formulation was revised and the matrix  $\|1/\varepsilon\|$  in Eqs. (28) and (29) was replaced by  $\|\varepsilon\|^{-1}$ . However only insignificant improvement in convergence was obtained [13].

The new formulation for unslanted gratings was recently suggested [11,12] where in Eq. (28)  $\|1/\varepsilon\|^{-1}$  and  $\|\varepsilon\|^{-1}$  are used instead of  $\|\varepsilon\|$  and  $\|1/\varepsilon\|$ , respectively. It means that inverse rule [16] is used, and in our notations in Eq. (27)

$$\mathbf{A} = \left\| \frac{1}{\varepsilon} \right\|^{-1}, \quad \mathbf{B} = 0, \quad \mathbf{G} = \|\varepsilon\|^{-1}. \quad (31)$$

This new formulation significantly improved the convergence of the method for metallic unslanted ( $\alpha = 0$ ) lamellar gratings for TM polarization. In this paper for slanted grating we will call formulation Eqs. (27) and (31) – “inverse” formulation.

Note that in formal way, Eq. (30) for the conventional formulation and Eq. (31) for the “inverse” formulation may be obtained from Eqs. (19) and (21) at  $s = 1, c = 0$  and at  $s = 0, c = 1$ , respectively.

#### 5. Numerical results

On the basis of the above presented theory a computer code was built. The computer code was written to accommodate the new FFFM based formulation and the conventional and “inverse” formulations also. The numerical results obtained from the code were compared with the results that are available in the

present literature for particular case of unslanted gratings in conical mountings [11,17] and with the results obtained by differential method [1] for slanted grating for TM polarization. Unfortunately, to our knowledge, for metallic slanted grating in conical mountings exact results are not available. Here we are therefore forced to use the “saturated” parts of the convergence curves to judge the convergence of various numerical implementations.

In order to investigate the convergence of the FFFM based modal method for metallic gratings, we consider an arbitrarily chosen gold lamellar grating etched on gold substrate with complex refractive index  $0.22 - i6.71$ . Linearly polarized plane wave is incident at an angle of incidence  $\theta = 30^\circ$  and at an azimuthal angle  $\delta = 30^\circ$  (Fig. 1). The incident medium is air. The electric-field vector is in the plane of incidence, so that angle  $\psi = 0$ . The grooves of the lamellar grating are slanted at angle  $\alpha = -45^\circ$ , the fill-in ratio (the duty cycle) of the grating is 0.5. The grating has a thickness  $b = 0.3 \mu\text{m}$ . The incident (vacuum) wavelength is  $\lambda = 0.8 \mu\text{m}$ , and the grating period is  $\Lambda = 0.7071 \mu\text{m}$ .

Figs. 2 and 3 show the convergence of the diffraction efficiencies as  $N$  increases, where  $2N + 1$  denotes the total number of space harmonics retained in Rayleigh expansions. The integer  $N$  is henceforth called the truncation order. We present two figures for the same grating in order to show in details the convergence curves frequently oscillating at  $N < 30$ . Fig. 2 shows the convergence of the zero-order diffraction efficiencies computed by modal method with the FFFM based formulation (filled circles and solid curve), with the conventional formulation (filled triangles and dash-dotted curve), and with the “inverse” formulation (crosses and dotted curve) as  $N$  increasing from 2 until 30.

The numerical results for the convergence of the zero-order and first-order diffraction efficiencies are shown in Fig. 3 for  $N$  increases from 2 to 100.

For both diffracted orders, the efficiencies computed with the FFFM based formulation converge remarkably quickly as  $N$  increases. For the conventional and “inverse” formulations the results of calculations oscillate and converge very slowly; in fact, they do not begin converging until  $N > 60$ . We may see from Table 1 and Fig. 3 that the FFFM formulation with  $N = 9$  (19 retained orders) provides more accurate results than the conventional and “inverse” formulations with  $N = 100$  (201 retained orders).

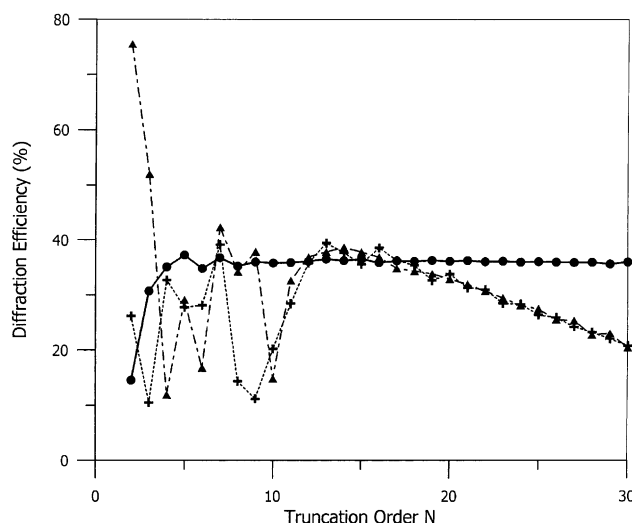


Fig. 2. Convergence of the zero-order diffraction efficiencies computed by modal method with the FFFM based formulation (filled circles and solid curve), with the conventional formulation (filled triangles and dash-dotted curve), and with the “inverse” formulation (crosses and dotted curve).

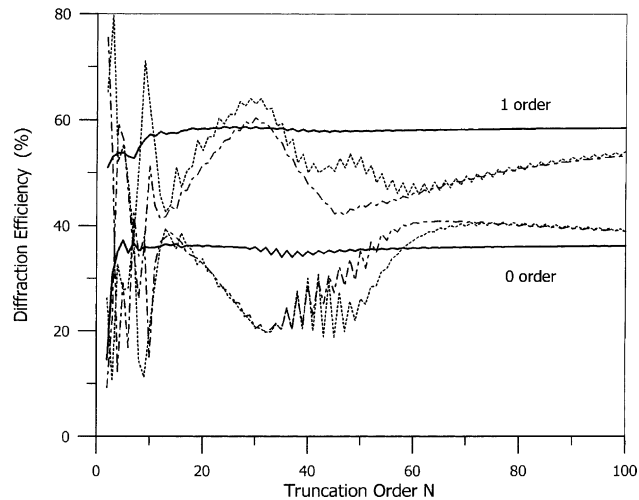


Fig. 3. Convergence of the zero-order and first-order diffraction efficiencies computed by modal method with the FFFM based formulation (—), with the conventional formulation (---), and with the “inverse” formulation (···).

Table 1

Numerical values of the first-order diffraction efficiencies (%) computed by modal method with different formulations

$N$	FFFM based formulation	“Inverse” formulation	Conventional formulation
9	56.366	71.091	36.557
40	57.777	50.043	47.865
50	57.831	53.060	43.922
60	58.049	47.950	46.128
70	58.187	49.434	48.930
80	58.324	51.450	50.928
90	58.411	52.968	52.328
100	58.491	54.039	53.351

In this table,  $N$  is the truncation order. The grating is etched on metallic substrate with complex refractive index  $0.22 - i6.71$ . The grooves of the lamellar grating are slanted at angle  $\alpha = -45^\circ$ , the fill-in ratio of the grating is 0.5, the grating period is  $A = 0.7071 \mu\text{m}$  and the thickness  $b = 0.3 \mu\text{m}$ . Linearly polarized plane wave is incident at an angle of incidence  $\theta = 30^\circ$  and at an azimuthal angle  $\delta = 30^\circ$ , the incident (vacuum) wavelength is  $\lambda = 0.8 \mu\text{m}$ . The electric-field vector is in the plane of incidence, so that angle  $\psi = 0$ .

## 6. Conclusion

A new formulation of the FMM that applies the rules of FFFM for slanted-fringe gratings in conical mountings has been presented. The new formulation leads to a convergence everywhere, and although the FFFM based formulation, the conventional and “inverse” formulations are rigorous at the limit of infinite series, a great difference appears at the numerical implementation level. The numerical results have convincingly shown that the FFFM based formulation of the eigenproblem provides highly improved convergence rates for metallic slanted gratings in the planar and conical mountings.

## References

- [1] E. Popov, M. Nevière, J. Opt. Soc. Am. A 17 (2000) 1773–1784.
- [2] L. Li, J. Opt. Soc. Am. A 14 (1997) 2758–2767.



- [3] C.B. Burckhardt, *J. Opt. Soc. Am.* 56 (1966) 1502–1509.
- [4] F.G. Kaspar, *J. Opt. Soc. Am.* 63 (1973) 37–45.
- [5] K. Knop, *J. Opt. Soc. Am.* 68 (1978) 1206–1210.
- [6] E. Noponen, J. Turunen, *J. Opt. Soc. Am. A* 11 (1994) 2494–2502.
- [7] K. Rokushima, J. Yamakita, *J. Opt. Soc. Am.* 73 (1983) 901–908.
- [8] M.G. Moharam, T.K. Gaylord, *J. Opt. Soc. Am.* 73 (1983) 1105–1112.
- [9] L. Li, C.W. Haggans, *J. Opt. Soc. Am. A* 10 (1993) 1184–1189.
- [10] M.G. Moharam, E.B. Grann, D.A. Pommet, T.K. Gaylord, *J. Opt. Soc. Am. A* 12 (1995) 1068–1086.
- [11] P. Lalanne, G.M. Morris, *J. Opt. Soc. Am. A* 13 (1996) 779–784.
- [12] G. Granet, B. Guizal, *J. Opt. Soc. Am. A* 13 (1996) 1019–1023.
- [13] P. Lalanne, *J. Opt. Soc. Am. A* 14 (1997) 1592–1598.
- [14] E.I. Krupitsky, B.C. Chernov, *Proc. IX All-Union School of Holography (in Russian)*, Leningrad, 1977, pp. 84–95.
- [15] B.C. Chernov, E.I. Krupitsky, *Proc. SPIE* 1183 (1990) 632–642.
- [16] L. Li, *J. Opt. Soc. Am. A* 13 (1996) 1870–1876.
- [17] L. Li, *J. Mod. Opt.* 40 (1993) 553–573.